LANGMUIR

pubs.acs.org/Langmuir Article

Self-Propelled Water Drops on Bare Glass Substrates in Air: Fast, Controllable, and Easy Transport Powered by Surfactants

Pauline E. Galy, Sergii Rudiuk, Mathieu Morel, and Damien Baigl*

Cite This: https://dx.doi.org/10.1021/acs.langmuir.9b03727 Read Online

ACCESS | Metrics & More | Article Recommendations | Supporting Information

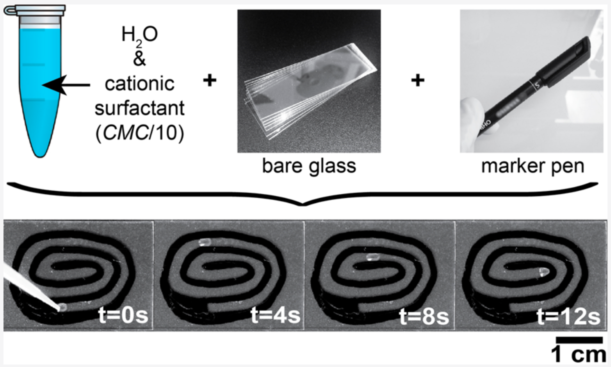

ABSTRACT: Self-propelled drops are capable of motion without external intervention. As such, they constitute attractive entities for fundamental investigations in active soft matter, hydrodynamics, and surface sciences, as well as promising systems for autonomous microfluidic operations. In contrast with most of the examples relying on organic drops or specifically treated substrates, here we describe the first system of nonreactive water drops in air that can propel themselves on a commercially available ordinary glass substrate that was used as received. This is achieved by exploiting the dynamic adsorption behavior of common *n*-alkyltrimethylammonium bromide (C_nTAB) surfactants added to the drop. We precisely analyze the drop motion for a broad series of surfactants carrying $n = 6$ to 18 carbon atoms in their tail and establish how the motion characteristics (speed, probability of motion) are tuned by both the hydrophobicity and the concentration of the surfactant. We show that motion occurs regardless of the n value but only in a specific concentration range with a maximum speed at around one tenth of the critical micelle concentration (CMC/10) for most of the tested surfactants. Surfactants of intermediate hydrophobicity are shown to be the best candidates to power drops that can move at a high speed (1−10 cm s^{-1}), the optimal performance being reached with $[C_{12}TAB] = 800\ \mu M$. We propose a mechanism where the motion originates from the anisotropic wettability of the substrate created by the electrostatic adsorption of surfactants beneath the moving drop. Simply drawing lines with a marker pen allows us to create guiding paths for drop motion and to achieve operations such as complex trajectory control, programmed drop fusion, drop refilling, as well as drop moving vertically against gravity. This work revisits the role of surfactants in dynamic wetting and self-propelled motion as well as brings an original strategy to build the future of microfluidics with lower-cost, simpler, and more autonomous portable devices that could be made available to everyone and everywhere.

■ INTRODUCTION

Miniaturization of chemical reactions has become a great challenge for the development of microanalysis devices and microchemical reactors. However, moving small quantities of fluid is often a tricky issue because of the increasing predominance of interfacial tension forces at smaller dimensions. During the past decades, the development of microfluidic technologies has allowed a precise control over fluid manipulation at the microscale.[1] However, these technologies often require multiple and complex fabrication steps as well as necessitate precise actuation devices such as pressure generators or electrode arrays. All these requirements make the approaches often costly, poorly portable, and easily prone to contamination. Having liquids compartmentalized into drops that could move by their own along user-defined pathways thus appears as an attractive solution to these limitations. Since the first reports in the early 90s,[2−6] the so-called self-propelled drops have constituted an attractive example of such system.

Self-propelled drop movement was observed on different kinds of substrates. This could involve a fluid interface, for instance in a liquid−liquid Leidenfrost-like system,[7] by dissolution of the drop[8] or the liquid marble[9] itself or by surfactant adsorption over the liquid interface,[10] especially with an alkaline ion gradient[11] or a pH gradient into the liquid.[12,13] Self-propelled drops were also reported to work because of a surfactant chemical modification inside themselves,[14−16] sometimes followed with the expulsion of oil vesicles in the aqueous bulk.[17,18] However, management of fluid interfaces may suffer from a lack of control accuracy because of the interface deformability and is always a challenge for applications as it

Special Issue: Advances in Active Materials

Received: December 3, 2019
Revised: February 19, 2020
Published: February 19, 2020

experimentally induces evaporation and transport issues. Researchers have thus actively looked for systems where drops could self-propel on solid substrates. This was typically achieved by using substrates with specifically modified surfaces, including surfaces with a wettability gradient for passive water drop propulsion[3,19−21] a pH gradient[22] or with a ratchet that allows thermal propulsion for Leidenfrost droplets.[23,24] Electrodes,[25,26] etching,[27] specific meltable substrates,[28] and adsorption on functionalized substrates[29,30] were also used for that purpose. However, all these systems require specific surfaces, limiting their range of applicability. A desired yet challenging alternative is thus to get drops self-propelling on bare glass substrates. This was achieved by generating wetting gradients through surface reactions on glass with organic[2,6,31] or liquid metal[32] drops and by subjecting oil drops to dynamic surfactant adsorption.[33,34] Although water is a solvent of choice for greener processes and biological investigations, to our knowledge, only one system with water-based drops propelling on bare glass has been reported. This was achieved through evaporation-induced surface tension gradients using two-component water drops of specific compositions.[35] In that case, an individual drop could not self-propel, and the motion was created only when another drop was present at its vicinity, leading to interesting yet complex collective behaviors. Here, we present an advantageous system where a single water drop can genuinely self-propel on bare glass slides in air without any external intervention. The key feature is the addition of cationic surfactants at a precise concentration, which upon electrostatic adsorption on the substrate creates an anisotropic wetting that efficiently propels the drop. Using common *n*-alkyltrimethylammonium bromide surfactants (C_nTAB) at different concentrations C_s, we precisely analyzed the drop movement using video recording, automated drop tracking, and high-speed imaging to systematically establish how the drop behavior depended on *n*, C_s, the substrate temperature, and the environment humidity. We also explored how these self-propelled drops could be easily supervised with minimal equipment to perform operations such as controlled trajectories, on-demand drop fusion, self-propelled vertical climbing, or drop refueling for long-term motion.

■ MATERIALS AND METHODS

Materials. Milli-Q water (Millipore, 18.2 MΩ·cm) was used for all experiments, and 76 mm × 26 mm glass slides (clear white glass, cut edges, Knittel) were used as received for all experiments unless otherwise specified. Hexyltrimethylammonium bromide (**C_6TAB**, CAS 2650-53-5, Sigma-Aldrich, purity >98.0%), octyltrimethylammonium bromide (**C_8TAB**, CAS 2083-68-3, Sigma-Aldrich, purity >98.0%), decyltrimethylammonium bromide (**C_{10}TAB**, CAS 2082-84-0, Sigma-Aldrich, purity >98.0%), dodecyltrimethylammonium bromide (**C_{12}TAB**, CAS 1119-94-4, Sigma-Aldrich, purity >98.0%), tetradecyltrimethylammonium bromide (**C_{14}TAB**, CAS 1119-97-7, Sigma-Aldrich, purity >98.0%), hexadecyltrimethylammonium bromide (**C_{16}TAB**, CAS 57-09-0, Sigma-Aldrich, purity >96.0%), and octadecyltrimethylammonium bromide (**C_{18}TAB**, CAS 1120-02-1, Sigma-Aldrich, purity >98%) were used as received.

Drop Deposition. All experiments were performed at 20 ± 3 °C and 31 ± 5% relative humidity unless otherwise specified. Each drop of studied solution was deposited on a glass slide with a 0.1−2.5 μL Eppendorf micropipet. A new glass slide face was used for each experiment.

Drop Motion of Bare Glass Slides. A 0.8 μL drop and a horizontal glass slide were used for each experiment (Figures 1−5).

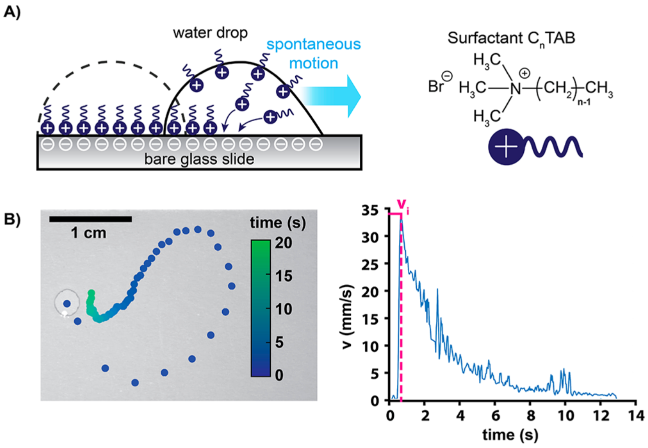

Figure 1. Self-propelled water drop on a bare glass slide. (A) A drop of water (left) containing *n*-alkyltrimethylammonium bromide surfactant (C_nTAB, right) is deposited on a bare glass slide. A spontaneous motion is observed for a range of concentrations depending on the surfactant chain length *n*. We hypothesize that the self-propelled motion is powered by the electrostatic adsorption of the cationic surfactant that creates a wetting gradient beneath the moving drop. (B, left) The representative trajectory of a 0.8 μL drop of water with [C_{12}TAB] = 800 μM. Colored disks correspond to the drop barycenter positions, as detected by a custom-built automated drop tracking system. The color code represents the time from deposition (blue) to the end of motion (green). (B, right) Instant drop speed (*v*) as a function of time for the trajectory shown on the left. After a short lag time, motion starts with a characteristic initial speed, noted v_i, and progressively slows down.

Drop Motion on Glass Slides Decorated with Tracks. Lines were manually drawn with a water-insoluble black pen (OHPen universal permanent black S 0.4 mm, Stabilo) to surround bare glass zones that were used as tracks for the drops. The drawn lines were left overnight for complete drying before use. For Figure 6E, a 2 μL drop of water containing C_{12}TAB (800 μM) was placed at the beginning of the track and was refilled regularly with addition of 0.6 μL of a concentrated C_{12}TAB solution (2 mM). For all other experiments, one (Figures 6A, 6B, 6D) or two (Figure 6C) 1 μL drop(s) of water containing C_{12}TAB (800 μM) was (were) deposited inside the desired track. All experiments were performed on horizontal slides except for Figure 6B, where the glass slide was placed against a support to form a 85° angle with respect to the horizontal plane.

Effect of Substrate Temperature and Environment Humidity. To analyze the effect of substrate temperature (Figure 2C), the glass slide was placed on a temperature-controlled aluminum surface (Dry Bath FB 15 103, Fisher Scientific) at the desired temperature. We waited 60 s prior to adding the drop on it. For the effect of humidity (Figure S6), the glass slides were placed inside a closed glass Petri dish containing a wet paper and let sit for 2 min to create a highly humid atmosphere. The drop was then deposited rapidly before the humidity chamber was closed again.

Video Recording. Real-time videos of the drop behavior were recorded with a digital reflex camera (5D Mark II, Canon) equipped with a 100 mm macro lens (Canon) at 29 frames per second. Camera control and movie acquisition was remotely achieved using the EOS Utility Software to avoid any mechanical perturbation during the experiment. The camera was placed parallel to the glass slide using a professional tripod (for all main figures except Figure 2C) or a custom-built holder for effect of temperature and humidity studies (Figures 2C, Figure S6). Ultrafast videos were recorded using a NX4 S1 camera (IDT) mounted with a 100 mm macro lens (Canon) at the frame rate indicated in the movie legend (Movies S6 and S7), using the Motion Inspector software.

Image Analysis and Drop Tracking. For Figures 1B, 2A, and 2B, the drop tracking was performed automatically using a custom-built Matlab script. Briefly, after detection of the slide edge by thresholding, the background was subtracted prior to detecting the

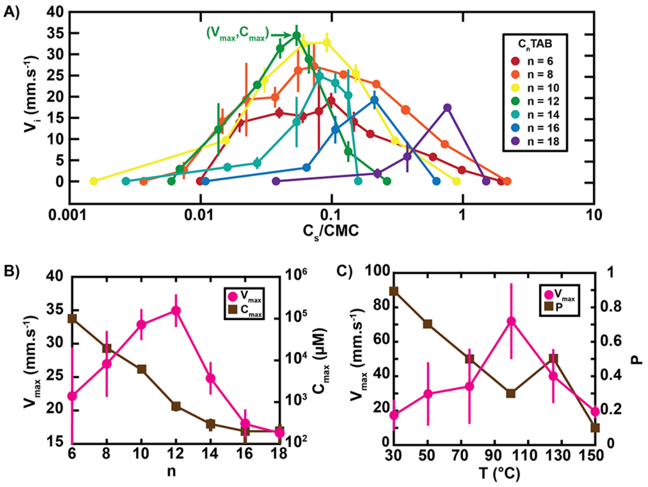

Figure 2. Drop speed analysis. (A, B) Experiments performed at a controlled temperature of 20 ± 3 °C and 31 ± 5% relative humidity. (A) Initial speed (v_i) as a function of surfactant concentration (C_s) normalized by the corresponding critical micelle concentration (CMC) for different carbon chain lengths (n = 6−18). For each surfactant, we observe a maximum speed (V_{max}) at the concentration noted C_{max}. (B) V_{max} (left axis, disk symbols) and C_{max} (right axis, square symbols) as a function of n. (C) V_{max} (left axis, disk symbols) and probability of motion (P, right axis, square symbols) as a function of the substrate temperature (T) for [C_{12}TAB] = 800 μM. All drops were 0.8 μL in volume. Symbols and error bars are mean values ± sd on 8 and 6 replicates in (A, B) and (C), respectively.

drop using an adapted threshold and extracting the coordinates of its center of mass by using the “regionprops” function. The frame-by-frame application of this treatment allowed to us to plot the drop position as a function of time (Figure 1B, left). For Figure 2C and Figure S6, the detection of the drop center was done frame by frame by using the “Manual Tracking” plugin from ImageJ.

Data Analysis. The drop center coordinates for two consecutive time points were used to calculate the instant speed as a function of time (Figure 1B, right). In the first instants, the drop contour underwent deformations, during which the measured speed was very erratic until it reached a stable shape that corresponded to the beginning of the motion. We took the first 5 velocities of this stable motion regime and averaged them to calculate a characteristic speed that is referred to as the initial speed (v_i) of the drop. This procedure was reproduced for the different surfactant concentrations, and we noted C_{max} as the concentration for which the mean initial velocity was maximum (noted V_{max}). The duration of motion and the distance followed by the drop were recorded as T_{motion} and d_{motion}, respectively. Each experiment was replicated 8 times unless otherwise specified, and values were given as the mean ± sd. The probability of motion (P) for given conditions was calculated by dividing the numbers of drop that actually moved over the total number of replicates.

■ RESULTS AND DISCUSSION

Our experiment consisted of the deposition of a 0.8 μL water drop on a bare glass slide that was used as received. When a proper concentration of an alkyltrimethylammonium bromide surfactant (C_nTAB, where n was the number of carbon atoms in the hydrophobic tail) was initially present in the drop, spontaneous drop motion was observed (Figure 1A, Movie S1). To our knowledge, this is the first time that spontaneous drop motion of a common aqueous solution is reported on an ordinary substrate which has not been specifically treated in advance for drop motion to occur (e.g., using a surface wettability gradient with surface chemistry,[3,19,21] pH gradient[15,22] or photocontrollable azobenzene monolayer[36]) and without chemical reaction (e.g., by etching the substrate[27]).

We tested different commercially available glass slides from different providers and found that the drop motion systematically occurred on some of them with a characteristic speed that depended on the slide type, while motion was not possible with others. Empirically, we noticed that the best candidates for self-propelled motion were hydrophilic glass slides for which water had an advancing contact angle in the range 5−15° (Figure S1). Substrates with a higher advancing contact angle refrained the drop from moving forward. Conversely, when the advancing angle was too low, a strong spreading of the drop hampered a consistent self-propelled motion. Interestingly, applying a localized plasma on a substrate that was initially too hydrophobic allowed us to define a hydrophilic path with a width comparable to the drop size. In that case, the drop was able to self-propel and progress along the path (Movie S2), even against gravity (Movie S3). We also tested the surface of other glass-based materials such as common laboratory glassware with a local plasma treatment. For instance, motion was reproducibly observed on glass Petri dishes (Movie S4). We thus conclude that (i) the self-propelled motion occurred only when a proper hydrophilicity was achieved and (ii) pure water drops remained static on hydrophilic bare glass slides but spontaneously self-propelled when a proper concentration of C_nTAB was used. For the rest of the study, we thus kept one type of a commercially available glass slide (Knittel, see Materials and Methods) on which self-propelled motion was reproducibly observed, and we used this substrate as received, without any plasma or other treatments. We developed an automated drop tracking system which allowed us to extract the speed profile of each tracked drop (Figure 1B). For given conditions, the speed profile was reproducible with moderate differences from one experiment to the other (Figure S2). A typical motion proceeded as follows. As soon as the drop was placed in contact with the substrate, it underwent erratic deformations for a very short lag time prior to starting its motion at a high speed with a well-defined shape. Once in movement, the drop speed continuously decreased (Figure 1B, right) except in a few cases where the presence of a surface defect or the slide edge could induce an abrupt change of the speed profile.

We systematically performed this analysis for various experimental conditions, extracted the initial speed v_i, and plotted it as a function of surfactant chain length (n) and concentration (C_s) normalized by the critical micelle concentration (CMC) of each tested surfactant (Figure 2A). Remarkably, all curves displayed a similar dumbbell profile regardless of n, showing that motion was typically possible when C_s was between 0.01 × CMC and 1 × CMC, with a maximum speed V_{max} observed at a concentration $C_{max} \approx 0.1 \times$ CMC except for C_{18}TAB for which $C_{max} \approx$ CMC. The probability that the drop moved was also maximal around C_{max} and equaled one for most of the surfactants, while it strongly dropped for situations where the concentration was too low or too large (Figure S3). We attributed this common CMC dependence to the role of cooperative surfactant assembly, and since the optimal speed was observed at a lower value than the nominal CMC, we deduced a predominant role of the surfactant at the solid/water and/or water/air interface(s). Interestingly, motion was not observed on these surfaces with an anionic surfactant (sodium dodecyl sulfate, SDS) for all the tested concentrations (C_s/CMC ranging from 1.2 × 10^{-3} to

https://dx.doi.org/10.1021/acs.langmuir.9b03727

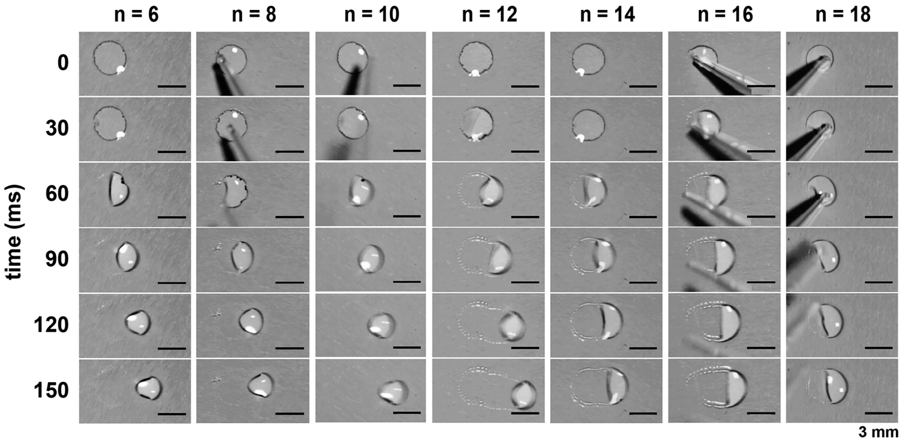

Figure 3. Drop behavior at the beginning of its motion. Timelapse images of a 0.8 μL drop at $C_s = C_{max}$ as a function of time, where $t = 0$ corresponds to the beginning of the motion, for various surfactant chain lengths (n). The pipet tip used for drop deposition is visible in some images. All scale bars are 3 mm.

1.2, Table S1), nor with drops containing a cationic surfactant (C_{12}TAB) on cationic substrates (Text S1). This shows that the sole surfactant behavior at the air/water interface, if it had an effect, was not enough to produce drop motion. Since self-propulsion was not observed with like-charged surfactant/substrate systems, we conclude that the electrostatic adsorption of cationic C_nTAB on the negatively charged glass substrate was instrumental in this process. This was confirmed by varying the ionic strength inside the drop. Progressively increasing the electrostatic screening by adding salt to the drop resulted in a strong and continuous decrease of both the speed and the range of C_s for motion to occur (Figure S4). With [NaCl] = 1 M, corresponding to a Debye length of ≈0.3 nm, the motion was totally inhibited. The surfactant electrostatic adsorption on the oppositely charged glass substrate resulted in the exposure of hydrophobic chains at the bottom of the drop. This in turn created a gradient of wettability that continuously propelled the drop toward the hydrophilic areas of the substrate where surfactants had not adsorbed yet. The proposed mechanism is reminiscent to that described for the very first reported self-running drops[2,6] but with electrostatic surfactant adsorption as a fuel hydrophobizing the substrate beneath the running drop instead of a surface chemical reaction. It also confirms the importance of the advancing contact angle on the substrate in this process (Figure S1). A low advancing contact angle was necessary for the wettability gradient induced by surfactant adsorption to be strong enough to ensure the drop motion, while a too hydrophilic substrate resulted in strong spreading of the drop hampering its motion. The existence of a maximum speed at an intermediate concentration was interpreted by antagonist effects of the dynamic adsorption of surfactants. For small amounts of surfactant, increasing C_s contributed to a higher hydrophobization of the glass substrate and therefore a stronger wettability gradient that promoted drop motion. In contrast, adding too much surfactant in the drop promoted the fast adsorption of surfactants into mono or potentially bi- or multilayered structures, resulting in reduced dynamic wettability gradients. Since the CMC decreases with an increase in surfactant hydrophobicity (Figure S5), the concentration C_{max} at which V_{max} was reached was strongly decreasing with an increase in surfactant chain length, from 0.1 M to 200 μM when n increased from 6 to 18 (Figure 2B). Interestingly, the largest values of V_{max} were obtained for surfactants of intermediate hydrophobicity, with the maximum (V_{max} = 34.7 ± 2.4 mm s^{-1}) being achieved for n = 12 (C_{max} = 800 μM), emphasizing again the role of the dynamic adsorption of surfactant at the water/substrate interface. Increasing n resulted in a stronger hydrophobization for a given rate of surfactant adsorption. Conversely, if for simplification, one neglects hydrodynamic effects and supposes that surfactants were mainly brought by diffusion to the substrate, increasing n also resulted in both lower working C_s (Figures 2A, 2B) and slower diffusion and, thus, in a decrease in the surfactant adsorption rate. These antagonist effects could explain the existence of the optimal propulsion observed for an intermediate value of n. We then fixed these optimal conditions ([C_{12}TAB] = 800 μM) and investigated the effect of the substrate temperature T (Figure 2C). Increasing T resulted in a decrease in motion probability and an increase in V_{max} to a maximum of 72.6 ± 22.1 mm s^{-1} at 100 °C. To determine whether these effects could be due to a stronger evaporation rate that could change the surfactant concentration in the drop, we performed a series of experiments at different temperatures under both normal (31 ± 5% relative humidity) and highly humid conditions. Interestingly, neither the speed, the probability, nor the distance of motion was significantly affected by the humidity conditions (Figure S6), showing that evaporation did not have a major role in controlling the drop transport. All these results show that the dynamic adsorption of cationic surfactants on the anionic glass substrate below the drops created a dynamical anisotropy in wettability that propelled the drop. As fuel for this self-propelled motion, the surfactants were consumed along the drop trajectory until motion stopped. At room temperature, the motion was typically maintained for around 5−10 s at the optimal surfactant concentration ($C_s \sim C_{max}$) (Figure S7).

To have better insights on this surfactant-powered self-propulsion, we observed the shape taken by the drop both at the beginning of and during its motion. First, we looked at the first moments of the drop motion at $C_s = C_{max}$ for all studied surfactants (Figure 3). Interestingly, we systematically observed an asymmetric retraction of the drop before its opposite contact line actually moved forward. Although the drop usually moved right after the contact line retraction, we occasionally observed a delay, allowing one to clearly

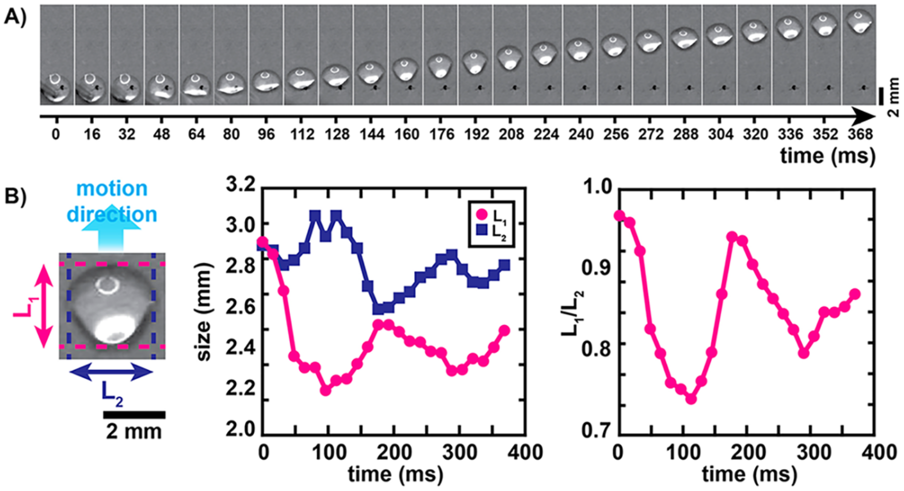

Figure 4. High-speed observation of a drop starting its motion. (A) Timelapse images of a 0.8 μL drop with $[C_{12}TAB]$ = 800 μM (C_{max}). The corresponding movie is displayed as Movie S6. (B) Length of the drop shown in (A) measured in a direction parallel (L_1) and perpendicular (L_2) to its motion and aspect ratio (L_1/L_2) as a function of time.

distinguish the two processes (Movie S5). This retraction shares analogy with the so-called autophobic effect where surfactants brought by the air−water interface at the contact line can induce a retraction of the contact line.[37−39] This was probably a key ingredient to create the initial wettability gradient to propel the drop away from the surfactant-enriched part of the substrate. Observed with a high-speed camera, the initial drop motion revealed a characteristic drop shape oscillation, in agreement with autophobic feeding of the drop rear by new surfactants and spreading at the front on the hydrophilic substrate (Figure 4, Movies S6−S7).

Although the initial motion started by a similar drop retraction into a crescent shape, different morphologies were observed during motion depending on the drop composition (Figure 5). All drops displayed an asymmetric shape with a similar front progressing on the naked glass, but they had strikingly different meniscus shapes at their back. The moving drops could be roughly categorized into two main morphologies, i.e., drops with a crescent-like shape for the most hydrophobic surfactants ($n \geq 14$) and comet-like drops for the more hydrophilic surfactants ($n \leq 10$). For the crescent-like morphology, the contact line kept retracting at the rear of the drop, probably by autophobic effect,[37−39] while for the comet-like drops, the back contact line was pulled by the moving drop and moved once its receding contact angle was reached. Interestingly, with the surfactant of intermediate hydrophobicity (n = 12) both shapes were observed, i.e., crescent-like for $C_s < C_{max}$ and comet-like for $C_s > C_{max}$.

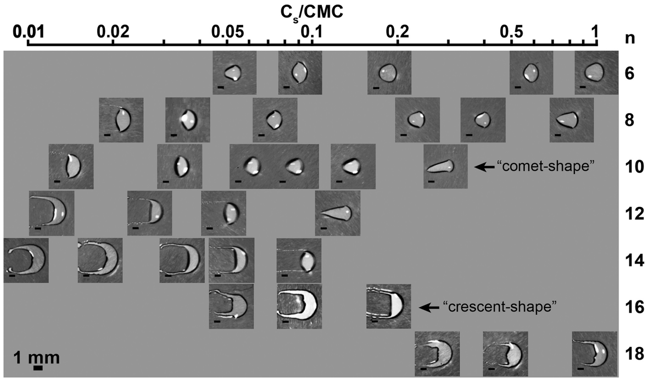

Figure 5. Surfactant chain length- and concentration-dependent shape of the self-propelled drop. Representative images of a 0.8 μL drop at v_i for various C_s/CMC and n values. Conditions are those of Figure 2A when drop motion was observed.

We then fixed the drop composition at which the highest speed was obtained at 25 °C (n = 12; C_{max} = 800 μM) and challenged its operability for user-defined, portable, and low-cost microfluidic operations, by privileging simple and heavy-instrument-free strategies. As for the movement study analysis, experiments were performed with the bare glass slides used as received without any cleaning or chemical treatment (plasma, silanization, etc.). When the drop was placed on the glass slide, it could move in any direction except that self-crossing trajectories were forbidden due to the presence of adsorbed surfactant left after the moving drop. To control the trajectory of the moving drop in a user-defined manner, we simply drew lines by hand with a permanent marker pen on the substrate and deposited the drop in the space between the drawn lines. Because the advancing contact angle at the hydrophobic ink location (103 ± 3°) became much larger than the typical range allowing for self-propulsion (5−15°, Figure S1), the lines behaved as barriers that drops could not cross, resulting in an efficient directed motion (Figure 6). Using parallel straight lines thus resulted in the perfectly straight trajectory of the drop between the lines. When the drop was deposited in the middle of the drawn track, it could start its motion in both directions but once the movement was initiated, the drop kept moving in the same direction as long as enough surfactant fuel was available and until it reached the stop line at the end of the track, where it stopped. When the drop was initially placed at the vicinity of a stop line, one direction became forbidden and the drop systematically moved away from the stop line, resulting in the perfect control of both the trajectory and the directionality of the motion (Figure 6A, Movie S8). This control was also efficient on almost vertical substrates, allowing efficient climbing of the drop on substrates inclined with an angle around 85° (Figure 6B, Movie S9). By simply placing one drop at the vicinity of each stop line of the same track, the control of trajectory and directionality of each drop toward each other allowed us to program their fusion in a reliable

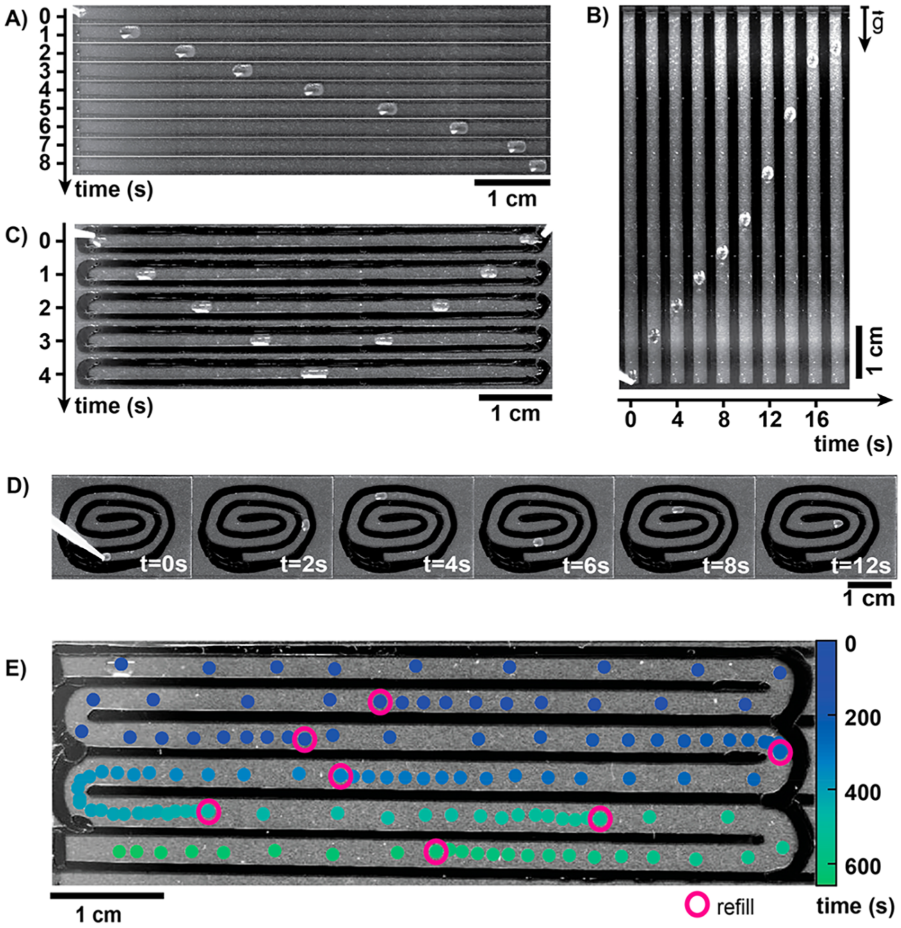

Figure 6. User-defined, low-cost drop operations. (A–D) Timelapse images of 1 μL water drops containing $[C_{12}TAB]$ = 800 μM (C_{max}) placed on a glass with lines previously hand-drawn with a permanent marker pen. (A) A single drop following a straight pathway on a horizontal substrate (Movie S8). (B) A single drop climbing along a quasi-vertical substrate (Movie S9). (C) The programmed fusion of two drops on a horizontal substrate (Movie S10). (D) A single drop following a curved pathway on a horizontal substrate (Movie S11). (E) Recorded position (disk symbols) every 4.8 s of a 2 μL drop initially containing $[C_{12}TAB]$ = 800 μM and refilled with 0.6 μL of $C_{12}TAB$ (2 mM) when indicated with a pink circle (Movie S13). The color of the disk symbol indicates the time after the drop deposition.

manner (Figure 6C, Movie S10). Controlled curved trajectories were obtained as well (Figure 6D, Movies S11–S12). In the absence of a stop line on its trajectory, the drop kept moving by consuming surfactants that adsorbed on the surface until the concentration became too low to sustain the motion. We thus explored the possibility of refueling the drop with surfactant. To this end, we placed a 2 μL drop in a track and let it self-propel until the motion nearly or fully stopped. Using a micropipet, we then added to the drop 0.6 μL of a 2 mM solution of $C_{12}TAB$ and observed that the drop recovered a high-speed self-propulsion (Figure 6E, Movie S13). We could successfully repeat this operation and make the drop move along a complex guiding track for a cumulative distance of about 42 cm. This principle could constitute the basis of a platform where drops could autonomously move over long periods of time by refueling themselves using reservoirs of concentrated surfactant solutions.

■ CONCLUSION

We have described a new principle for the self-propelled motion of a drop on a solid substrate in air. We showed that a water drop containing a cationic surfactant (C_nTAB) with a chain length having n = 6–18 carbon atoms efficiently self-propelled on a bare glass substrate when the proper surfactant concentration was used. Regardless of n, the optimal concentration resulting in the highest speed and highest probability of motion was found to be around CMC/10. Surfactants of intermediate hydrophobicity were shown to be the best candidates to power drop motion, with the optimal conditions (800 μM of $C_{12}TAB$) resulting in a speed of ~35 mm s^{-1} at room temperature. Our experiments revealed that the motion was due to the anisotropic wetting created by the electrostatic adsorption of surfactants at the interface between the substrate and the moving drop. The surfactant transport by the liquid–air interface toward the substrate seemed to contribute at the beginning of the motion through the so-called autophobic effect as well as during the motion, especially with surfactants of high hydrophobicity. Using tracks made by simply drawing lines on the glass slides, we efficiently guided the self-propelled drop motion along user-defined straight or curved trajectories, on both horizontal and vertical substrates, and made drops fuse on demand. Our system differs from what has been explored so far by several aspects, leading to interesting properties and performance. First, the drops described here are water based and therefore compatible with greener organic solvent-free operations as well with the transport or manipulation of biological components. Moreover, our approach does not involve any chemical reaction nor any specifically treated surface, making it particularly versatile and universal. Two drawbacks have to be mentioned, however. First, the performance of the transport is strongly dependent on the glass used. However, we have empirically found that glass slides offering an advancing contact of 5° to 15° allow efficient transport, making it possible to select, or design, appropriate substrates for self-propelled motion to occur. We also showed that glass slides with an initially too high advancing angle could be plasma treated so that, combined with hydrophobic barriers, controlled self-propelled motion was also obtained. The second limitation comes from the origin of the self-propelled mechanism. Since surfactants are deposited upon motion, (i) self-crossing trajectories cannot be achieved and (ii) the drop consumes surfactants to move and stops when the surfactant concentration becomes too small. The self-crossing avoidance can be seen in fact as an advantage as it is a robust way to maintain the drop directionality in guiding tracks while the surfactant consumption can be compensated by appropriate point refilling of the drop. Finally, our results demonstrate that with broadly available and cost-effective materials of extreme simplicity, a bare glass slide and a marker pen, self-propelled water drops powered by surfactants can be easily tamed as autonomously moving entities capable of user-defined operations such as controlled trajectories, on-demand drop fusion, and refueling. Overall, this work not only stimulates open questions on out-of-equilibrium transport, dynamic wetting, and capillary motion but also constitutes a valuable brick in the groundwork for the necessary construction of future microfluidic devices that would be more portable, cost-effective, and truly autonomous, with the ultimate objective to make it available to any citizen, regardless of his/her resources, wealth, geographic, or economic situation.

■ ASSOCIATED CONTENT

Supporting Information

The Supporting Information is available free of charge at https://pubs.acs.org/doi/10.1021/acs.langmuir.9b03727.

Figures S1−S7, Supplementary Table S1, Supplementary Text S1, and the legends of the movies (PDF)

Movie S1 (AVI)

Movie S2 (AVI)

Movie S3 (AVI)

Movie S4 (AVI)

Movie S5 (AVI)

Movie S6 (AVI)

Movie S7 (AVI)

Movie S8 (AVI)

Movie S9 (AVI)

Movie S10 (AVI)

Movie S11 (AVI)

Movie S12 (AVI)

Movie S13 (AVI)

■ AUTHOR INFORMATION

Corresponding Author

Damien Baigl − *PASTEUR, Department of Chemistry, École Normale Supérieure, PSL University, Sorbonne Université, CNRS 75005 Paris, France*; orcid.org/0000-0003-1772-3080; Email: damien.baigl@ens.fr

Authors

Pauline E. Galy − *PASTEUR, Department of Chemistry, École Normale Supérieure, PSL University, Sorbonne Université, CNRS 75005 Paris, France*

Sergii Rudiuk − *PASTEUR, Department of Chemistry, École Normale Supérieure, PSL University, Sorbonne Université, CNRS 75005 Paris, France*; orcid.org/0000-0003-1728-1163

Mathieu Morel − *PASTEUR, Department of Chemistry, École Normale Supérieure, PSL University, Sorbonne Université, CNRS 75005 Paris, France*; orcid.org/0000-0002-6284-1708

Complete contact information is available at: https://pubs.acs.org/10.1021/acs.langmuir.9b03727

Author Contributions

S.R. discovered the phenomenon in drops containing surfactant and DNA. P.E.G. performed all the experiments. Automated image analysis was developed by P.E.G. and M.M. D.B. supervised the work. P.E.G. and D.B. analyzed the data and wrote the manuscript with contributions from all authors. All authors have given approval to the final version of the manuscript.

Funding

We thank ENS for a student grant and Ph.D. funding (P.E.G.).

Notes

The authors declare no competing financial interest.

■ ACKNOWLEDGMENTS

We thank Koyomi Nakazawa (ENS) for help in the drops fusion experiment (movie S10); Colin D. Bain (Durham University) and Manos Anyfantakis (University of Luxembourg) for insightful discussions.

■ REFERENCES

(1) Whitesides, G. M. The Origins and the Future of Microfluidics. *Nature* **2006**, *442* (7101), 368−373.

(2) Bain, C. D.; Burnett-Hall, G. D.; Montgomerie, R. R. Rapid Motion of Liquid Drops. *Nature* **1994**, *372* (6505), 414−415.

(3) Chaudhury, M. K.; Whitesides, G. M. How to Make Water Run Uphill. *Science* **1992**, *256* (5063), 1539−1541.

(4) Brochard-Wyart, F.; De Gennes, P. G. Spontaneous Motion of a Reactive Droplet. *C. R. Acad. Sci.* **1995**, 285−288.

(5) Shanahan, M. E.R.; de Gennes, P.-G. Start-up of a Reactive Droplet. *C. R. Acad. Sci., Ser. IIb: Mec., Phys., Chim., Astron.* **1997**, *324*, 261−268.

(6) Dos Santos, F.; Ondarçuhu, T. Free-Running Droplets. *Phys. Rev. Lett.* **1995**, *75* (16), 2972−2975.

(7) Janssens, S. D.; Koizumi, S.; Fried, E. Behavior of Self-Propelled Acetone Droplets in a Leidenfrost State on Liquid Substrates. *Phys. Fluids* **2017**, *29* (3), 032103.

(8) Nagai, K.; Sumino, Y.; Kitahata, H.; Yoshikawa, K. Mode Selection in the Spontaneous Motion of an Alcohol Droplet. *Phys. Rev. E* **2005**, *71* (6), 1−4.

(9) Bormashenko, E.; Frenkel, M.; Bormashenko, Y.; Chaniel, G.; Valtsifer, V.; Binks, B. P. Superposition of Translational and Rotational Motions under Self-Propulsion of Liquid Marbles Filled with Aqueous Solutions of Camphor. *Langmuir* **2017**, *33* (46), 13234−13241.

(10) Ban, T.; Kita, T.; Tominaga, H.; Shioi, A. Droplet Motion Induced by Spontaneous Breaking of Flow Symmetry in Aqueous Two-Phase Systems. *Chem. Lett.* **2008**, *37* (2), 162−163.

(11) Ban, T.; Nakata, H. Metal-Ion-Dependent Motion of Self-Propelled Droplets Due to the Marangoni Effect. *J. Phys. Chem. B* **2015**, *119* (23), 7100−7105.

(12) Francis, W.; Fay, C.; Florea, L.; Diamond, D. Self-Propelled Chemotactic Ionic Liquid Droplets- Suporting Material. *Chem. Commun.* **2015**, *51* (12), 2342−2344.
(13) Miura, S.; Banno, T.; Tonooka, T.; Osaki, T.; Takeuchi, S.; Toyota, T. PH-Induced Motion Control of Self-Propelled Oil Droplets Using a Hydrolyzable Gemini Cationic Surfactant. *Langmuir* **2014**, *30* (27), 7977−7985.
(14) Hanczyc, M. M.; Toyota, T.; Ikegami, T.; Packard, N.; Sugawara, T. Fatty Acid Chemistry at the Oil-Water Interface: Self-Propelled Oil Droplets. *J. Am. Chem. Soc.* **2007**, *129* (5), 9386−9391.
(15) Banno, T.; Kuroha, R.; Toyota, T. PH-Sensitive Self-Propelled Motion of Oil Droplets in the Presence of Cationic Surfactants Containing Hydrolyzable Ester Linkages. *Langmuir* **2012**, *28* (2), 1190−1195.
(16) Thutupalli, S.; Seemann, R.; Herminghaus, S. Swarming Behavior of Simple Model Squirmers. *New J. Phys.* **2011**, *13*, 073021.
(17) Hanczyc, M. M.; Toyota, T.; Maru, N.; Sugawara, T.; Ikegami, T. Self-Propelled Oil Droplets Consuming "Fuel" Surfactant. *J. Am. Chem. Soc.* **2009**, *131* (14), 5012−5013.
(18) Sugawara, T.; Takakura, K.; Toyota, T.; Tsuha, H.; Yamada, K.; Ikegami, T. Listeria -like Motion of Oil Droplets. *Chem. Lett.* **2006**, *35* (7), 708−709.
(19) Kooij, E. S.; Zandvliet, H. J. W.; Poelsema, B.; Jansen, H. P.; Bliznyuk, O. Smart Design of Stripe-Patterned Gradient Surfaces to Control Droplet Motion. *Langmuir* **2011**, *27* (17), 11238−11245.
(20) Chakraborty, M.; Ghosh, U. U.; Chakraborty, S.; Dasgupta, S. Thermally Enhanced Self-Propelled Droplet Motion on Gradient Surfaces. *RSC Adv.* **2015**, *5* (56), 45266−45275.
(21) Li, J.; Tian, X.; Perros, A. P.; Franssila, S.; Jokinen, V. Self-Propelling and Positioning of Droplets Using Continuous Topography Gradient Surface. *Adv. Mater. Interfaces* **2014**, *1* (3), 1400001.
(22) Lagzi, I.; Soh, S.; Wesson, P. J.; Browne, K. P.; Grzybowski, B. A. Maze Solving by Chemotactic Droplets. *J. Am. Chem. Soc.* **2010**, *132*, 1198−1199.
(23) Linke, H.; Alemán, B. J.; Melling, L. D.; Taormina, M. J.; Francis, M. J.; Dow-Hygelund, C. C.; Narayanan, V.; Taylor, R. P.; Stout, A. Self-Propelled Leidenfrost Droplets. *Phys. Rev. Lett.* **2006**, *96* (15), 2−5.
(24) Lagubeau, G.; Le Merrer, M.; Clanet, C.; Quéré, D. Leidenfrost on a Ratchet. *Nat. Phys.* **2011**, *7* (5), 395−398.
(25) Nakanishi, S.; Nagai, T.; Ihara, D.; Nakato, Y. Self-Propelled Oil Droplets on Metal Surfaces during Electrodeposition. *ChemPhysChem* **2008**, *9* (16), 2302−2304.
(26) Kuge, T.; Ishibashi, Y.; Mukouyama, Y.; Fukuda, Y.; Yae, S.; Nakanishi, S.; Yamada, Y. Self-Propelled Motion of a Nitrobenzene Droplet on Au Electrode during Sn Electrodeposition: Factors Creating Imbalance of Interfacial Tension and Marangoni Effect. *J. Electrochem. Soc.* **2018**, *165* (9), H473−H480.
(27) Li, J.; Yao, X.; Zhou, D.; Jiang, L.; Bai, H.; Zhang, H.; Ju, J.; Yang, B. Running Droplet of Interfacial Chemical Reaction Flow. *Soft Matter* **2012**, *8* (22), 5988.
(28) Lazar, P.; Riegler, H. Reversible Self-Propelled Droplet Movement: A New Driving Mechanism. *Phys. Rev. Lett.* **2005**, *95* (13), 1−4.
(29) Lee, S.-W.; Laibinis, P. E. Directed Movement of Liquids on Patterned Surfaces Using Noncovalent Molecular Adsorption. *J. Am. Chem. Soc.* **2000**, *122* (22), 5395−5396.
(30) Lee, S.-W.; Kwok, D. Y.; Laibinis, P. E. Chemical Influences on Adsorption-Mediated Self-Propelled Drop Movement. *Phys. Rev. E: Stat. Phys., Plasmas, Fluids, Relat. Interdiscip. Top.* **2002**, *65* (5), 051602.
(31) Brochard-Wyart, F.; Ondarçuhu, T.; Cuvelier, D.; Beaune, G.; Douezan, S.; Dufour, S.; Murrell, M. P.; Sens, P.; Dumond, J.; Blanch-Mercader, C.; et al. Spontaneous Migration of Cellular Aggregates from Giant Keratocytes to Running Spheroids. *Proc. Natl. Acad. Sci. U. S. A.* **2018**, *115* (51), 12926−12931.
(32) Zhang, J.; Yao, Y.; Sheng, L.; Liu, J. Self-Fueled Biomimetic Liquid Metal Mollusk. *Adv. Mater.* **2015**, *27* (16), 2648−2655.
(33) Sumino, Y.; Magome, N.; Hamada, T.; Yoshikawa, K. Self-Running Droplet: Emergence of Regular Motion from Nonequilibrium Noise. *Phys. Rev. Lett.* **2005**, *94* (6), 068301.
(34) Nanzai, B.; Ishikawa, R.; Igawa, M. Spontaneous Motion of O-Toluidine Droplets: Repetitive Motion of Running and Squashing. *Chem. Lett.* **2012**, *41* (6), 609−611.
(35) Cira, N. J.; Benusiglio, A.; Prakash, M. Vapour-Mediated Sensing and Motility in Two-Component Droplets. *Nature* **2015**, *519* (7544), 446−450.
(36) Oh, S.-K.; Nakagawa, M.; Ichimura, K. Photocontrol of Liquid Motion on an Azobenzene Monolayer. *J. Mater. Chem.* **2002**, *12*, 2262−2269.
(37) Tadmor, R.; Baksi, A.; Gulec, S.; Jadhav, S.; N'guessan, H. E.; Sen, K.; Somasi, V.; Tadmor, M.; Wasnik, P.; Yadav, S. Drops That Change Their Mind: Spontaneous Reversal from Spreading to Retraction. *Langmuir* **2019**, *35* (48), 15734−15738.
(38) Frank, B.; Garoff, S. Surfactant Self-Assembly near Contact Lines: Control of Advancing Surfactant Solutions. *Colloids Surf., A* **1996**, *116* (1−2), 31−42.
(39) Frank, B.; Garoff, S. Origins of the Complex Motion of Advancing Surfactant Solutions. *Langmuir* **1995**, *11* (1), 87−93.

https://dx.doi.org/10.1021/acs.langmuir.9b03727
Langmuir XXXX, XXX, XXX−XXX